Lateral Behaviour of Velocity and Turbulence Characteristics in Open Channels with Submerged Heterogeneous Bed

Olatunji Peter Folorunso and James Olugbenga Aribisala
School of Civil Engineering, University of Birmingham, Edgbaston, B15 2TT, Birmingham, United Kingdom

Corresponding Author:
Olatunji Peter Folorunso
School of Civil Engineering, University of Birmingham, Edgbaston, B15 2TT, Birmingham, United Kingdom

Abstract: Most open channels are not comprised of uniform boundary roughness but instead in any given cross section consist of different roughness with varying frictional surface resistance, this heterogeneous bed roughness is ubiquitous in natural rivers and often influence and control the mean and turbulent flow structures in open channels thereby impacting on the conveyance capacity. This study describes the interaction of flexible vegetation and gravel bed on the mean and turbulent flow characteristics of an idealized heterogeneous open channel modelled using Astroturf (as grass vegetation) and gravel, the bed interaction is established alternately at both sides of the flume to form a partly vegetated open channel in a checkerboard pattern under a fully submerged condition. Mean velocities and turbulent properties are measured using the Acoustic Doppler Velocimeter (ADV). From the measured data, the cross sectional distribution of velocity and turbulent properties are obtained. The study shows flow concentration at the free surface and a reduced mean flow near bed over the grass bed. Estimated pattern of secondary flow reveals the interaction between the two bed roughness. The primary source of velocity shear as the dominant cause of the increased Reynolds shear stresses and turbulent activities occurred over the grass bed.

INTRODUCTION

Natural rivers and open channels are characterized by hydraulic and morphology complexities, this is due to the existence of several interconnected physical features like boundary roughness, vegetation, geometry[1] etc. Their mutual interaction often affects the flow characteristics of open channel systems[2]. In order to estimate the conveyance capacity of natural open channels, it is necessary to understand the flow-feature interactions at multiple scales, how it affects the relevant transport processes and subsequently the physical impacts the flow interactions can have on the environment[3]. The physical features present in the open channel system can be evaluated as the resistance parameters associated with the channel system. Accurate estimation of these parameters

in both river morphology changes and hydraulic characteristics of flow (i.e., the local velocities and depths of flow) are necessary for the restoration and protection of biodiversity[4].

The importance of the vegetated zone in rivers has been acknowledged for river management and environmental benefits; therefore, vegetation has been recognized and encouraged in river channels to provide restoration and stability processes to balance the ecosystem. Moreover, it is necessary to mitigate the flow resistance due to restoration to reduce the risk of flooding[1].

A number of researchers have experimentally and numerically investigated the effects of vegetation on turbulence properties in open channel flow, e.g.[1-3, 5, 6]. However, the structure and interaction of flows in partly vegetated open channels simultaneously with other bed roughness has not been investigated.

In spite of the widespread research on vegetated channel flows, there exists a gap in understanding the mechanism of vegetation interaction with other bed roughness, e.g., gravel in terms of turbulence production, dissipative effect and exchange mechanism, these are key issues for successful river restoration and flood management programmes. A better understanding of this interaction will help to better understand the complex hydrodynamic system of natural rivers and channels for providing adequate flood management in river restoration processes. In this study, the effect of submerged flexible vegetation and gravel bed interactions on turbulent flow characteristics is investigated.

MATERIALS AND METHODS

Laboratory experiments were conducted in a 22 m long and 0.614 m wide straight rectangular glass wall flume at the Civil Engineering Laboratory University of Birmingham Fig. 1 and 2. The flume channel is fed with water from a constant head located at the laboratory roof. The discharge is measured by an electronic gauge installed in the discharge pipe. The channel tailgate outlet is controlled by the rolling system, allowing its height to be set to achieve a normal depth flow. Needle pointer gauges in centre line of the flume were used to measure water depths. The experimental channel defines a maximum friction factor f = 0.159271 and Manning's sn = 0.025. Table 1 showing the geometric parameter of the flume for the flow:

Table 1: Flume and flow parameters

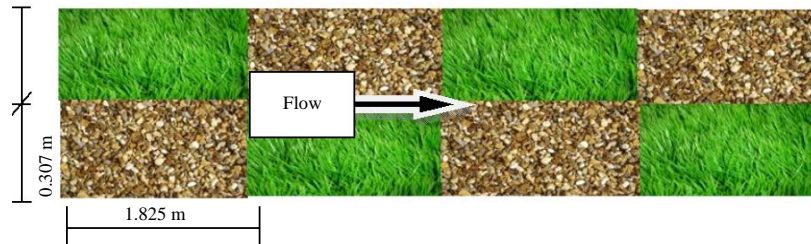| Q (l/sec)	H (mm)	R_e	F_r	n_{max}	f_{max}
29.50	135⊙	3.31×10^5	0.30	0.025	0.159271

Fig. 1: Channel bed plan configuration

Fig. 2: Flume channel bed roughness variations and grass plant consisting 16 stems

The flume bed was modelled using Astroturf (to represent grass vegetation) and gravel, the model beds were alternated to form a checkerboard configuration[7] (Fig. 1). The bed roughness surface was set to allow negligible variation in bed surface elevation. Bed roughness changes at every 1.825 m as illustrated in Fig. 1. The measurement cross section is located 18m downstream the flume inlet, the experiment was conducted at uniform fully developed turbulent flow conditions. Measuring using digital Caliper Vernier with accuracy 0.01, the stem height, width and thickness of the modelled grass are found to be 30, 1 and 0.15 mm, respectively, each plant consists of 16 stems joined together to form a bunch of 2.3 mm diameter Fig. 2, the coverage areal density of the grass bed is 15625 plants/m^{2}[6]. The gravel bed was created with fine gravels having $D_{70} = 10$ mm and $D_{4} = 5$ mm, packed densely and fixed to the channel bed by means of waterproof adhesive.

Velocity was sampled using the Acoustic Doppler Velocimeter (ADV) and Pitot-static tube at 10 mm vertical and horizontal spacing. Due to the restriction of the ADV, Pitot-static tube was used to measure the free surface region of the flow[8]. 3D velocity measurements were conducted at each sampling location using the ADV with maximum frequency 200Hz for a period of 60 sec in the velocity range 0.30 m/sec and with the accuracy of 0.06%[9]. The sampling volume was equal to 7.0 mm. The flow discharge was fixed at 29.50 L/sec and the corresponding uniform flow depth given as 135 mm which gives the average width (614 mm) to depth ratio (B/H) as 4.5. The three component velocities were sampled over a cross section located at 18m downstream the channel inlet.

The time series were despiked using the[9] Modified Phase-Space Threshold algorithm. To correct for probe misalignment, axis rotation by batch method[7] was applied. Mean and turbulence properties were calculated for each measured location. The ADV data was processed using the MAJ's velocity analyzer[8].

RESULTS AND DISCUSSION

Mean velocity profile and distribution: An essential aspect of the experiment is to ensure that the flow was uniform. Figure 3 shows that the upstream velocity profiles are similar to the profile at the measured cross section; the velocity profiles are negligibly different along the longitudinal direction. This is an indication that the flow was fully developed at the measured section while Fig. 4 shows the vertical distribution of the mean velocity for each bed in comparison to gravel side, the figure shows near bed flow deceleration and free surface acceleration on the grass side.
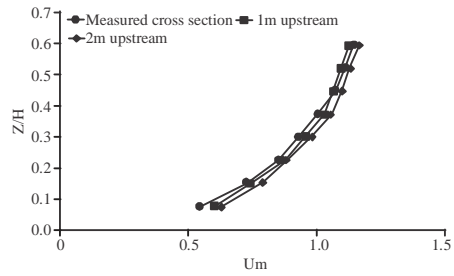

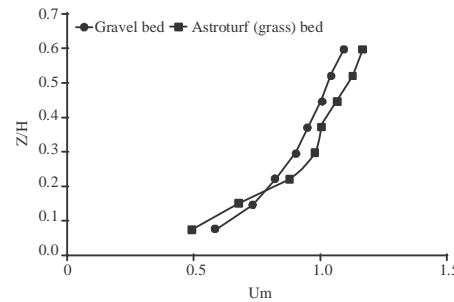Fig. 3: Mid-point vertical profiles of mean velocity in streamwise direction

Fig. 4: Vertical profiles of mean velocity over grass and gravel bed

Table 2: The channel mean streamwise velocities

$U_{Q/A}$ (m sec^{-1})	U_{i} (m sec^{-1})	Difference (%)
0.355	0.349	1.8

The distribution of mean velocity (U_{m}) normalized by the channel orifice mean velocity $(U_{Q/A})$ is shown in Fig. 5; this includes velocities measured with the Pitot-static tube. The gravel bed extends the region $\leq y/B < 0.5$ and the grass bed spanning $0.5 \leq y/B \leq 1.0$. The integrated channel mean velocity U_{i} (as measured) and the orifice mean velocity obtained from discharge Q and flow cross-sectional area A as $U_{Q/A} = Q/A$ are given in Table 2. The difference between the two mean velocities (U) is found to be $< 1.8\%$, this verifies the consistency of the measuring instruments.

Figure 5 suggests that the mean velocity distribution near bed shows pattern relative to the bed roughness combination, the middle flow are more symmetrical, the maximum mean velocity appears at the free surface and progressively reduces towards the channel bed as would be expected. The near bed $(z/H \leq 0.3)$ mean velocities are higher over the gravel side $0 \leq y/B < 0.5$ than the grass side $0.5 \leq y/B \leq 1.0$ in contrary, the streamwise mean velocities attain maximum over the grass side, this can be attributed to the fact that due to the bed configuration the high velocity flow is transported from the gravel region to the grass region, the flow decelerates near bed as it switches to the grass bed with subsequent flow concentration and by continuity accelerate near the free surface leading to a high streamwise velocity.
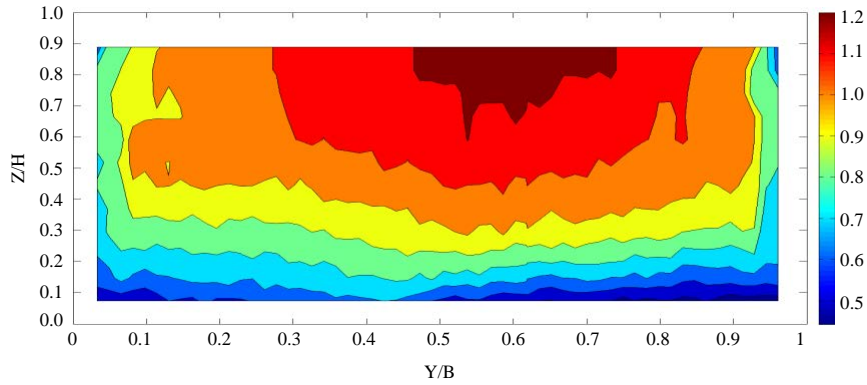
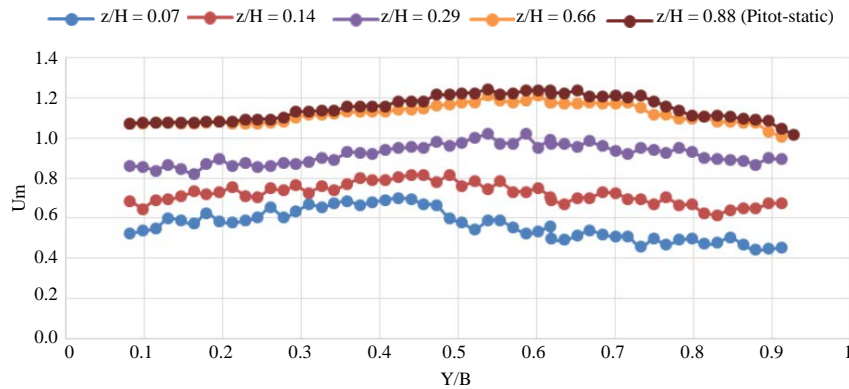Fig. 5: Relative normalized U_m distribution

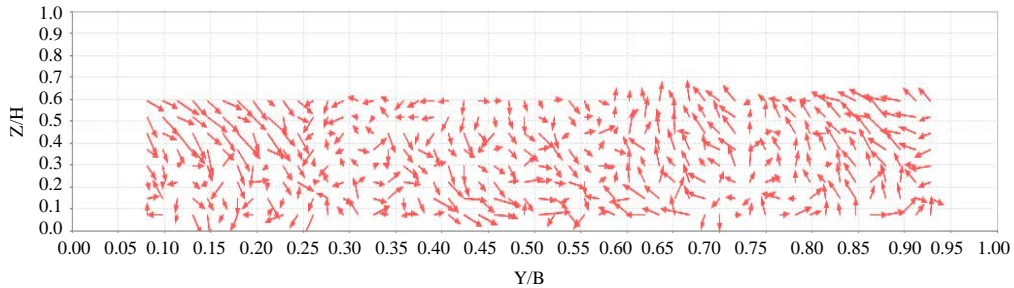Fig. 6: Lateral distribution of relative mean velocity

Fig. 7: Secondary flow distribution

The lateral distributions of the mean velocity for selected heights is shown in Fig. 6, closer to the channel bed, the lateral profiles have asymmetric distribution, it is more regular at the upper region of the flow. The lateral profile shows that minimum and maximum mean velocities occurred over the grass bed. At z/H = 0.07, the mean velocity is greater on the gravel side ($0 \leq y/B \leq 0.5$) while at z/H ≥ 0.29 the mean velocity is also found to be greater over the grass side.

Secondary flow: The lateral and vertical components of the mean velocities were merged to obtain the secondary vectors $(\sqrt{V^2+W^2})$. The integrated magnitude of the

vector is close to zero with the Root Mean Square (RMS) of the maximum measured mean vector found to be 1.2% of the mean streamwise velocity[7]. Figure 7 shows the lateral distribution of the secondary flow, the figure shows the directions of the secondary flow with downflow occurring over the gravel bed $0 \leq y/B < 0.5$ and upflow over the grass bed $0.5 \leq y/B \leq 1.0$, the depicting downward movement close the gravel sidewall ($0.15 \leq y/B \leq 0.25$) can be said to be formed at the corners due to non uniformity in the wall turbulence[10]. The secondary flow moves upward the low velocity fluid on grass bed and transport same to the gravel side near the free surface while downflow occurs on gravel side which
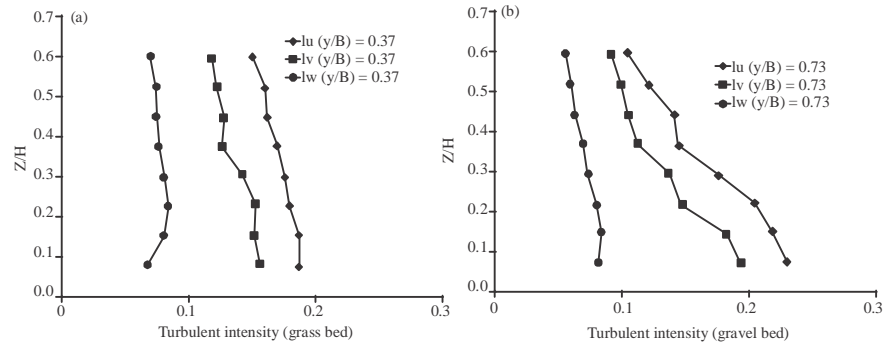
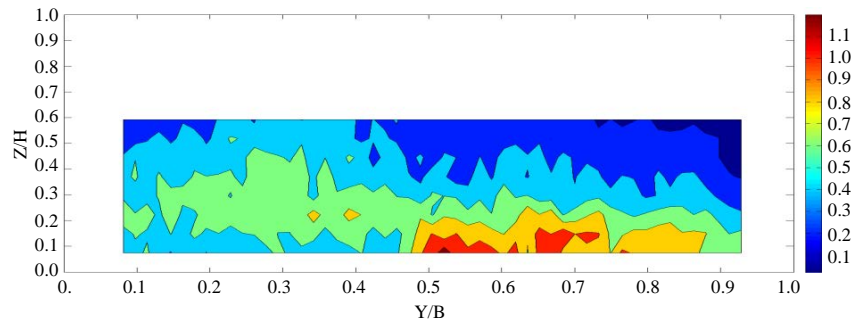Fig. 8: Vertical distribution of turbulent intensities

Fig. 9: Relative distribution of vertical reynolds stress $\left(-\rho\overline{u'w'}\right)$

transport the high velocity fluid near the free surface down the lower portion of the flow, at this region the fluid is transported laterally into the grass bed, the upflow on grass side is an effect of the near bed retardation caused by grass stems prompting low velocity fluid, for continuity the low velocity fluid is moved upward by the secondary flow and directs same towards the gravel side. The secondary flow indicates that, at the lower portion of the flow, the transverse motion is directed from the gravel bed to the grass bed, transporting the high velocity fluid from gravel bed towards grass bed, while at the upper portion, the low velocity fluid generated on grass bed moves up and transported laterally in the opposite direction.

The effects of secondary flow on the streamwise velocity can be seen in Fig. 5, at the lower portion of the flow the isovels slopes downward from both sides of the bed towards the center of the channel ($0.35 \leq y/B \leq 0.48$) this corresponds to a region where downward flow is substantial Fig. 7. The slopes define the condition that secondary currents transport fluids from both sides of the channel towards the channel center and the interface region. At the channel near bed, the mean streamwise velocity U_m region approximately ($0.6 \leq y/B \leq 0.9$) corresponds to region of upflow where the streamwise isovels swells up. The isovel lines are deflected down at approximately ($0.35 \leq y/B \leq 0.48$) which forms the region of downflow.

Table 3: Integrated channel mean turbulent intensities

I_u	I_v	I_w
0.166	0.133	0.073

Turbulent intensity: Table 3 shows the integrated magnitude of the turbulent intensities I_u, I_v and I_w in which $I_u = \delta_u/U$, $I_v = \delta_v/U$ and $I_w = \delta_w/U$. The magnitude of the vertical turbulent intensity I_w is significantly lower than the streamwise I_u and lateral I_v turbulent intensities with the results showing that $I_u > I_v > I_w$ as shown in Table 3.

The vertical distributions of turbulent intensities are shown in Fig. 8, it can be seen that vertical turbulent intensity (I_w) is significantly lower than the remaining components. The figures show that vertical turbulent intensity remains approximately constant near the free surface and decreases towards the bottom of the channel. This is an indication of both the free surface and channel bed damping of vertical fluctuations.

The minimum streamwise I_u and lateral I_v turbulent intensities are found to be at the free surface and increases linearly away from the free surface to the channel bed. It is found that the streamwise turbulent intensity I_u attains maximum over the grass bed where as the vertical turbulent intensity seem to be of the same order for both beds.

Reynolds stresses: Figure 9 shows the distribution of the vertical Reynolds Stress $\left(-\rho\overline{u'w'}\right)$ which is normalized by the
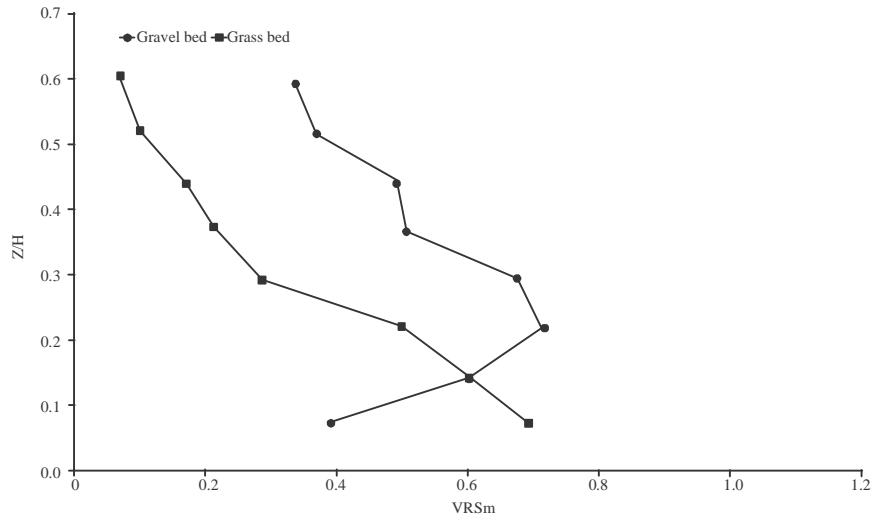
Fig. 10: Vertical Distribution of Relative Vertical Reynolds Stress by Bed
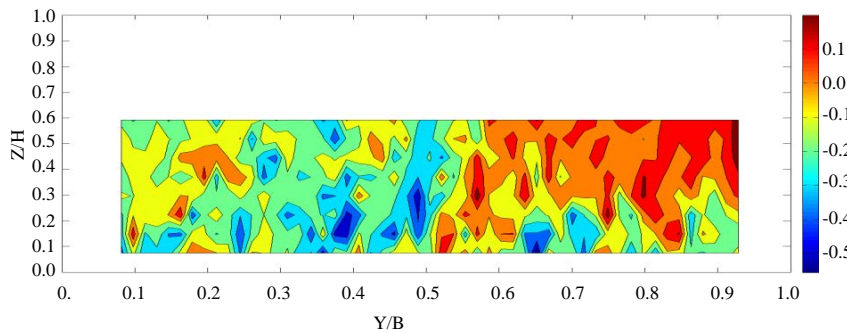

Fig. 11: Relative Distribution of Horizontal Reynolds Stress

channel mean bed shear stress ($pgRS_0$). The vertical Reynolds stress attains a maximum value over the grass bed in the region ($0.50 < y/B < 0.8$) with $\left(-\rho\overline{u'w'}\right)$ decreasing as the flow depth increases. There is an evidence of negative vertical Reynolds stresss $\left(-\rho\overline{u'w'}\right)$ in the upper region of the flow on the grass side.

The vertical distribution of $\left(-\rho\overline{u'w'}\right)$ is shown in Figure 10 for the channel beds. On grass bed ($0.5 \leq y/B \leq 1.0$) the vertical Reynolds stress $\left(-\rho\overline{u'w'}\right)$ is linear with a maximum value at the bed and decreases linearly with flow depth towards the free surface. On gravel bed ($0 \leq y/B \leq 0.5$), the vertical Reynolds stresss $\left(-\rho\overline{u'w'}\right)$ has a local maximum above bed approximately ($z/H \cong 0.2$) and decay linearly towards the channel bed and the free surface from the maximum point. The range ($z/H \cong 0.2$) agrees with the wall region as defined by Nakagawa and Nezu[11]. In this region the $\left(-\rho\overline{u'w'}\right)$ decreases towards the channel bed due to the presence of significant viscous shear stress induced by the bed roughness at the wall region[12]. This contributes to momentum balance in the near bed flow region due to the dissipation through viscous forces. Meanwhile such feature is not observed on grass bed

suggesting that, the inner and wall region with form and viscous stress is located below the roughness crest due to semi-permeable nature of the grass bed.

Figure 11 shows the cross sectional distribution of horizontal Reynolds stress $\left(-\rho\overline{u'v'}\right)$. It may be seen that the maximum $\left(-\rho\overline{u'v'}\right)$ appears on grass bed near the free surface (Nezu and Sanjou, 2008). The horizontal vortices generated by the shear layer is transported to the free surface by the secondary flow Figure 7. The stress spreading across the grass bed to the centre is apparent. On gravel bed, the horizontal Reynolds stress $\left(-\rho\overline{u'v'}\right)$ is of negative magnitude relative to grass bed as confirmed in Fig. 12.

Comparing Fig. 11 with Fig. 7, it may be seen that the region of maximum $\left(-\rho\overline{u'v'}\right)$ corresponds with the upflow region where horizontal vortices are transported to the free surface and Fig. 9 shows that the corresponding $\left(-\rho\overline{u'w'}\right)$ values are negative in the region where $\left(-\rho\overline{u'v'}\right)$ hare large, confirming a momentum balance as described by (Shiono and Knight, 1991). There is an indication of horizontal shear layer dominating over the grass bed.
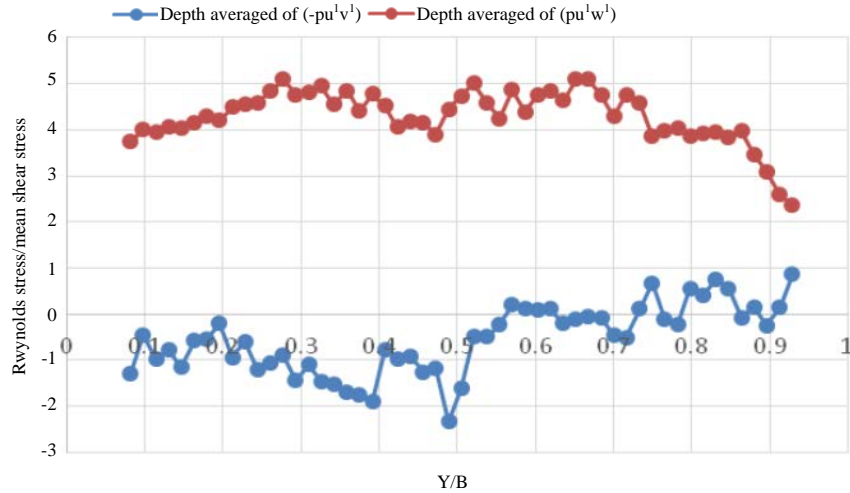
Fig. 12: Depth Averaged Reynolds Stress ($\left(-\rho\overline{u'v'}\right)$ and $\left(-\rho\overline{u'w'}\right)$)

CONCLUSION

This study studies the mean and turbulent behaviour in a uniform open channel flow with flexible vegetation partly fixed with gravel bed in a rectangular open channel. The study is characterized by a lateral variability of all the time averaged flow quantities over a region extending up to 35% of the water depth from the channel bed. The response of the flow over the grass bed includes attenuation of the mean streamwise velocity near bed, flow concentration and high streamwise velocity at the free surface. The secondary flow provides a mechanism for momentum transfer with downflow observed over the gravel bed and upflow over the grass bed, the pattern of secondary current indicates that flow is transported at the upper region on grass side and subsequently at the lower region on gravel side. Turbulent intensities are roughness dependent close to the channel bed and subsequently vary near bed; it is observed from the bed resistance that the form drag is smaller in gravel than in grass roughness. The maximum horizontal Reynolds stress occurs over the grass bed indicating a horizontal shear over the grass bed. This may be responsible for the additional turbulent activities noticed over the grass bed.

NOTATION

- b: Channel width (mm)
- h: Flow Depth
- x, y, z: streamwise, lateral and vertical velocity components
- I_u, I_v, I_w: streamwise, lateral and vertical turbulent intensities x, y, z axes
- $\left(-\rho\overline{u'v'}\right)$: Mean Horizontal Reynolds Stress
- $\left(-\rho\overline{u'w'}\right)$: Mean Vertical Reynolds Stress
- U_m: Mean streamwise velocity

- U_i: Integrated streamwise channel mean velocity value
- Q: Flow discharge
- A: Cross sectional Area
- R_e: Reynolds number
- F_r: Froude number

REFERENCES

01. Nepf, H.M. and E.R. Vivoni, 2000. Flow structure in depth limited, vegetated flow. J. Geophys. Res. Oceans, 105: 28547-28557.
02. Righetti, M., 2008. Flow analysis in a channel with flexible vegetation using double-averaging method. Acta Geophys., 56: 801-823.
03. Velasco, D., A. Bateman, J.M. Redondo and V. DeMedina, 2003. An open channel flow experimental and theoretical study of resistance and turbulent characterization over flexible vegetated linings. Flow Turbul. Combust., 70: 69-88.
04. Termini, D., 2009. Experimental analysis of turbulence characteristics and flow conveyance effects in a vegetated channel. Proceedings of the International Conference on EGU General Assembly Abstracts Vol. 11, April 19-24, 2009, University of Palermo, Palermo, Italy, pp: 5792-5805.
05. Nezu, I. and M. Sanjou, 2008. Turburence structure and coherent motion in vegetated canopy open-channel flows. J. Hydro-Environ. Res., 2: 62-90.
06. Okamoto, T.A. and I. Nezu, 2009. Turbulence structure and Monami phenomena in flexible vegetated open-channel flows. J. Hydraul. Res., 47: 798-810.
07. Jesson, M., 2011. The effect of heterogeneous roughness on conveyance capacity and application to the Shiono-Knight Method. Ph.D Thesis, University of Birmingham, Birmingham, UK.

08. Jesson, M., 2013. MAJ's velocity signal analyser. Free Software Foundation, Boston, Massachusetts, USA. http://webcache.googleusercontent. com/search?q=cache:4IDcD8VDmmUJ:www.mike jesson.com/DataAnalyserWebsite/downloads/MAJ VSA_Installation_and_User_Guide.pdf+&cd=1&hl= en&ct=clnk&gl=pk

09. Goring, D.G. and V.I. Nikora, 2002. Despiking acoustic doppler velocimeter data. J. Hydraul. Eng., 128: 117-126.

10. Perkins, H.J., 2006. The formation of streamwise vorticity in turbulent flow. J. Fluid Mech., 44: 721-740.

11. Nakagawa, H. and I. Nezu, 1993. Turbulence in Open Channel Flows. Taylor & Francis, Abingdon, UK., ISBN:9789054101185, Pages: 293.

12. Nezu, I. and K. Onitsuka, 2001. Turbulent structures in partly vegetated open-channel flows with LDA and PI V measurements. J. Hydraul. Res., 39: 629-642.